Determination of Membrane Immersion Depth with O_2: A High-Pressure ^{19}F NMR Study

R. Scott Prosser,* Paul A. Luchette,* Philip W. Westerman,† Annett Rozek,‡ and Robert E. W. Hancock‡
*Department of Chemistry, Kent State University, Kent, Ohio 44242, and †Northeastern Ohio Universities' College of Medicine, Rootstown, Ohio 44272 USA; and ‡Department of Microbiology and Immunology, University of British Columbia, Vancouver, British Columbia V6T 1Z3, Canada

ABSTRACT Oxygen is known to partition with an increasing concentration gradient toward the hydrophobic membrane interior. At partial pressures (P_{O2}) of 100 Atm or more, this concentration gradient is sufficient to induce paramagnetic effects that depend sensitively on membrane immersion depth. This effect is demonstrated for the fluorine nucleus by depth-dependent paramagnetic shifts and spin-lattice relaxation rates, using a fluorinated detergent, $CF3(CF_2)_5C_2H_4$-O-maltose (TFOM), reconstituted into a lipid bilayer model membrane system. To interpret the spin-lattice relaxation rates (R_1^P) in terms of a precise immersion depth, two specifically fluorinated cholesterol species (6-fluorocholesterol and 25-fluorocholesterol), whose membrane immersion depths were independently estimated, were studied by ^{19}F NMR. The paramagnetic relaxation rates, R_1^P, of the cholesterol species were then used to parameterize a Gaussian profile that directly relates R_1^P to immersion depth z. This same Gaussian curve could then be used to determine the membrane immersion depth of all six fluorinated chain positions of TFOM and of two adjacent residues of specifically fluorinated analogs of the antibacterial peptide indolicidin. The potential of this method for determination of immersion depth and topology of membrane proteins is discussed.

INTRODUCTION

The extent of immersion depth of specific labels in lipid bilayers is critical to our understanding of the interaction of small organic molecules, drugs, and proteins with membranes. Information regarding immersion depth and topology of membrane proteins is also important to properly interpret three-dimensional membrane protein structure determined by high-resolution solution NMR in detergent micelles or solid-state (SS) NMR in bilayers. Membrane immersion depth is commonly measured by low-angle diffraction techniques (Knott and Schoenborn, 1986; Caffrey and Wang, 1995; Katsaras, 1995; McIntosh, 1999; Lohner and Prenner, 1999) or electron spin resonance (ESR) (Altenbach et al., 1990, 1994; Hubbell and Altenbach, 1994; Steinhoff et al., 1995; Hubbell et al., 1996). In this paper, we present a new means to reliably determine membrane immersion depth by NMR. The technique is based on the property that the paramagnetic influence of oxygen on a fluorine nucleus depends sensitively on membrane immersion depth and that this effect dominates spin-lattice relaxation rates and chemical shift changes at high pressures. The technique is demonstrated by ^{19}F NMR of specifically fluorinated cholesterol (6-fluorocholesterol (6FCH) and 25-fluorocholesterol (25FCH)), a semiperfluorinated test compound ($CF3(CF_2)_5C_2H_4$-O-maltose (TFOM)), and an isotopically fluorinated membrane peptide (indolicidin), all of which insert into the lipid bilayer.

Three-dimensional structures of membrane peptides may be determined by standard high-resolution NMR methods in detergent micelles. These methods include experiments designed to identify spin groups and assign resonances, in addition to experiments, such as the nuclear Overhauser effect spectroscopy (NOESY), which effectively measure through-space spin-spin connectivities (Jeener et al., 1979; Cavanagh et al., 1996). Heteronuclear (indirect-detect) high-resolution NMR experiments, which make use of large one- or two-bond scalar couplings in uniformly ^{13}C- and ^{15}N-labeled proteins, effectively improve spectral resolution and sequential assignment of resonances, extending the size limit for high-resolution NMR studies of membrane proteins (Cavanagh et al., 1996; Becker, 2000). The positioning and topology of the protein in the membrane is then frequently determined by identifying NOEs with lipid or detergent peaks. Alternatively, positioning can be identified using NMR by introducing depth-specific nitroxide spin labels and water-soluble shift reagents (Brown et al., 1982; Esposito et al., 1992; Franklin et al., 1994; Papavoine et al., 1995; Chupin et al., 1995). Within distances of 25 Å from an unpaired electron, the nuclear spin-lattice and spin-spin relaxation rates will be affected through the dipolar paramagnetic interaction. This interaction depends on the inverse sixth power of the separation between the nuclear and electron spins. This principle can be applied to the determination of positioning and topology of membrane proteins by NMR, using paramagnetic oxygen, rather than the nitroxide spin labels, as a probe. The advantages of such an approach will be discussed later in this paper.

ESR spectroscopy, in combination with site-directed spin labeling, also makes use of oxygen to determine immersion depth and topology of membrane proteins (Altenbach et al.,

Received for publication 3 August 2000 and in final form 29 November 2000.

Address reprint requests to Dr. R. Scott Prosser, Department of Chemistry, Williams Hall, Kent State University, Kent, OH 44242. Tel.: 330-672-9524; Fax: 330-672-3816; E-mail: sprosser@membrane.kent.edu.

0006-3495/01/03/1406/11 $2.00

1990). A spin-labeled derivative is first attached to a single cysteine residue in the protein or its mutant. ESR spectra and saturation decay rates are very sensitive to water-soluble shift reagents (i.e., Ni(II)ethylenediaminediacetate or Ni(II)acetylacetonate) and apolar (membrane-soluble) oxygen. By measuring ESR spectra and decay rates in the presence of these contrasting paramagnetic species, the positioning of a given spin label can be reliably determined in the membrane. For example, by performing a series of such measurements on a membrane channel protein, in which each residue is separately replaced with the spin-labeled derivative, it is possible to map out immersion depth and exposure to the inside of the channel, or outside membrane environment, for each residue (Altenbach et al., 1990). In this way, the topology and approximate three-dimensional structure of the membrane protein can then be determined.

Oxygen is an ideal paramagnetic probe for membrane immersion studies by NMR. In general, the dipolar expressions for paramagnetic shifts and spin-lattice relaxation times are straightforward to interpret in terms of exposure to oxygen or relative immersion depth. Because the paramagnetic contribution to the spin-lattice relaxation rate depends on the square of the gyromagnetic ratio, it stands to reason that ^{1}H or ^{19}F NMR studies should be most sensitive to oxygen. ^{19}F NMR chemical shifts, which span nearly 1000 ppm, are also particularly sensitive to paramagnetic additives (Gerig, 1994; Danielson, and Falke, 1996). Therefore, we have chosen to investigate the potential of membrane immersion studies with paramagnetic oxygen, using ^{19}F NMR, though the technique should certainly be applicable to other nuclei. As in the above ESR studies, it should in general be important to employ a water-soluble paramagnetic shift reagent to determine the degree (if any) to which the label of interest is accessible to solvent. There is a long history of such studies, using ^{19}F NMR. In some cases, chemical shift changes can be observed from solvent-accessible ^{19}F-labeled sites, simply by exchanging D_2O for H_2O (Sykes and Hull, 1978; Dettman et al., 1982). In other cases, paramagnetic additives have been shown to exert a significant effect on the ^{19}F chemical shifts of solvent-accessible sites.

In contrast to membrane immersion studies by ESR using site-directed mutagenesis, ^{19}F labels give rise to almost no structural or electrostatic perturbations and have very little influence on enzyme activity (Gerig, 1994; Danielson, and Falke, 1996). Furthermore, due to the extensive chemical shift range, multiple ^{19}F labels can be considered in a single membrane immersion and topology study. For example, a variety of fluorinated residues can be incorporated biosynthetically and nearly fully expressed (Gerig, 1994; Danielson, and Falke, 1996). Alternatively, in a manner similar to that described above for site-directed ESR spin labeling, fluorinated substituents, such as trifluoroethylthio (TET) may be readily attached to the sulfhydryl groups of cysteine residues, under nondenaturing conditions. Fluorine labels such as TET are unquestionably smaller and, therefore, less perturbing than comparable ESR spin labels. This would be expected to result in more uniform activities for site-directed mutants of membrane proteins. Recently, we demonstrated that relative immersion depth of specifically fluorinated species in membrane-associated molecules could be determined from ^{19}F spin-lattice relaxation times or chemical shifts in the presence of oxygen at partial pressures of 20 Atm (Prosser et al., 2000). These depth-dependent paramagnetic effects depend on local oxygen concentration, and in this paper we show that at higher pressures the oxygen concentration gradient is significantly increased, resulting in improved depth resolution at pressures of 100 Atm or more. Using ESR data, which approximated the oxygen-diffusible accessibility as a function of membrane immersion depth (Windrem and Plachy, 1980), we also quantitatively interpret the ^{19}F paramagnetic spin-lattice relaxation rates, R_1^P, in terms of membrane immersion depth, for a given composition, in an isotropic bicelle (vide infra). The relevant paramagnetic expressions and necessary theory are first introduced, and some detail to experimental methods associated with NMR in the presence of oxygen at high pressures is given. The method is demonstrated using a small semiperfluorinated test compound, two isotopically fluorinated cholesterol species, and an isotopically fluorinated antibacterial peptide, which is known to insert into membranes. Finally, the potential of the above NMR membrane immersion studies for topology and three-dimensional structure studies of membrane proteins is discussed.

MATERIALS AND METHODS

The (3,3,4,4,5,5,6,6,7,7,8,8,8)tridecylfluoro β-D-octylmaltoside (TFOM) was a gift from C. Sanders (Case Western Reserve University, Cleveland, OH). The 15% (w/v) bicellar dispersions consisting of phospholipid, 1,2-dimyristoyl-*sn*-glycero-3-phosphocholine (DMPC) and detergent, 1,2-dihexanoyl-*sn*-glycero-3-phosphocholine (DHPC), were prepared in 99.9% D_2O (Isotec, Miamisburg, OH). DMPC/DHPC molar ratios (referred to hereafter as q) of 0.5 were used. Typically, TFOM (2–5 mg) was combined with DMPC/DHPC (~250 mg) giving a DMPC/TFOM molar ratio of between 20 and 50. The samples were vortexed, followed by a few cycles of freeze thawing and centrifuging, after which a clear solution was obtained. The monofluorinated sterols, 6-fluorocholesterol (6FCH) and 25-fluorocholesterol (25FCH), were synthesized by fluorination of the 6-keto group of 6-ketocholestanol-3-acetate and the 25-hydroxy group of 25-hydroxycholesteryl-3-acetate by diethylaminosulfur trifluoride (Harte et al., 1996; Dauber et al., 1985). High-resolution ^{19}F, ^{13}C, and ^{1}H NMR confirmed molecular identity. Bicelle samples containing 6FCH and 25FCH were prepared by first co-dissolving the lipids and cholesterol species in methanol/chloroform (70/30, v/v). The solvent was removed by rotary evaporation, and the sample was then rehydrated and mixed until clear. The sample consisted of approximately 2.6 mg of 6FCH and 25FCH, corresponding to a DMPC/cholesterol ratio of approximately 30:1. All lipids (DMPC and DHPC) were obtained from Avanti Polar Lipids (Alabaster, AL). 5F-L-tryptophan was obtained from Fluka (Milwaukee, WI) and used to prepare a specifically fluorinated peptide, indolicidin. The backbone terminal amide group was protected with Fmoc chloride, and the indole nitrogen was protected with a CBZ protecting group to prevent cross-linking during solid-phase peptide synthesis. The indolicidin analogs,

ILPWKWP[5F-W]WPWRR-NH_2 and ILPWKWPW[5F-W]PWRR-NH_2, were prepared by the Nucleic Acid/Peptide Synthesis (NAPS) facility at the University of British Columbia. Peptide purity was confirmed by HPLC and mass spectroscopy. The peptide was added to an isotropic bicelle mixture. The lipid-to-peptide ratio was estimated to be 55, whereas the DMPC-to-DHPC ratio was 1.

High-pressure experiments were performed using a 5-mm OD (3.5-mm ID) sapphire tube (Saphikon, NH). A 1/4-inch copper tube sleeve was fitted over the end of the tube, which was in turn fitted into a standard 1/4-inch Swagelok nut, as shown in Fig. 1. The NMR tube, sleeve, and nut were epoxied together using 4000-psi epoxy, and the Swagelok nut was in turn connected to a reducer and a 1/8-inch Swagelok nut and tubing. The tubing remained connected through a three-way valve to a high-pressure gauge and oxygen tank during the NMR experiment. The sample was routinely pressurized outside the magnet for at least 36 h. One very important component in high-pressure experiments with oxygen is the sample plug, as shown in Fig. 1. Note that the inner surface of the sample plug is curved so that a small volume of air remains above the liquid during pressurization. The plug also contains a small hole through which the sample may be injected or withdrawn, using a 0.8-mm (OD) 8-inch syringe. In the absence of this plug, at high partial oxygen pressures we observed the gas to displace the liquid as the sample was lowered into the magnet. This was not observed when we pressurized the sample with nitrogen, and we attribute this effect to magnetic forces acting on the oxygen gas as the sample is lowered into the magnet.

^{19}F NMR experiments were performed on a Varian INOVA 500-MHz high-resolution spectrometer, by tuning the proton channel of a 5-mm probe to the ^{19}F resonance frequency (470.327 MHz). All experiments were performed at 40°C, where DMPC is expected to adopt bilayer domains within the isotropic bicelle sample. Spin-lattice relaxation times were measured by a simple inversion-recovery sequence $\{\pi-\tau-\pi/2-\text{acquire}\}$, using a repetition time of 3.5 s at ambient pressure and 1 s at high pressure. At least 16 τ values were used to characterize the inversion-recovery decay curves. All of the decay curves proved to fit very well to single exponentials. ^{19}F $\pi/2$ pulse lengths were 5.2 μs. A spectral width of 32 kHz and acquisition time of 250 ms were used, with a delay of 100 μs after the last pulse, preceding acquisition. Spectra were usually processed with 2–20 Hz line broadening and referenced to an internal standard of trifluoroacetic acid (−76.55 ppm). T_1 relaxation times and line widths were measured using Varian software.

RESULTS AND DISCUSSION

Bicelles as model membranes for solid-state and high-resolution NMR

Bilayered micelles, or bicelles, are a convenient model membrane system to study the feasibility of the membrane immersion depth experiments, either by solid-state (SS) or high-resolution solution NMR (Sanders and Prosser, 1998). If a mixture of a long-chain phospholipid, such as DMPC, and a short-chain phospholipid, such as DHPC, is prepared such that the molar ratio of long-chain lipid to short-chain lipid (i.e., q) is 2.8, a stable aggregate results consisting of a DMPC-rich bilayer domain surrounded by an annulus of DHPC (Ram and Prestegard, 1988; Sanders and Prestegard, 1990; Sanders and Schwonek, 1992; Sanders et al., 1994). At temperatures between 37°C and 43°C these bicelles are observed to align in magnetic fields, giving well-resolved SS NMR spectra. If the molar ratio q is reduced to between 1.0 and 0.5, the bicelles no longer align and the NMR spectrum is observed to be isotropic and suitable for high-resolution NMR studies (Vold et al., 1997).

For purposes of demonstrating membrane immersion and topology experiments by NMR, the bulk of the studies presented in this paper make use of $q = 0.5$ (isotropic) bicelles. This system has the advantage that sensitivity is improved over oriented bicelle systems, whereas rf-power requirements are easily achieved without the necessity of ^{1}H decoupling. However, the proposed method is equally applicable in oriented bicelles and other model membrane systems and appears to be more sensitive in model membrane systems with low detergent concentrations (i.e., $q =$ 2.8 bicelles and unilamellar vesicles). Recent ^{19}F NMR experiments on 5-fluorotryptophan in aligned bicelles revealed minimal line broadening and downfield shifts, induced by oxygen at 100 Atm P_{O2}, on the order of 3 ppm (data not shown).

Probing immersion depth with fluorinated amphiphiles

Recently, the semiperfluorinated membrane detergent TFOM, shown in Fig. 2 *A*, was used to probe relative immersion depth in isotropic bicelles and model membranes (Prosser et al., 2000). TFOM, which is readily solubilized in the isotropic bicelle, is expected to anchor into the membrane, such that the fluorines at positions 3 through 8 would be progressively immersed in the membrane interior. In an effort to quantitatively interpret the depth-dependent paramagnetic relaxation rates in terms of membrane immersion depth, we have also employed cholesterol (CH), separately

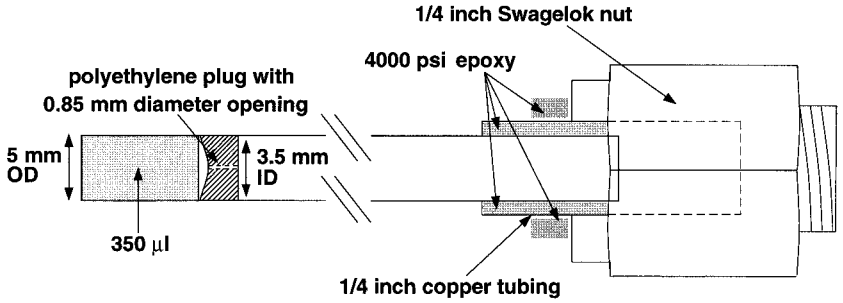

FIGURE 1 The sapphire NMR tube, internal plug, and connection to a 1/4-inch Swagelok nut, used in the high-pressure experiments.

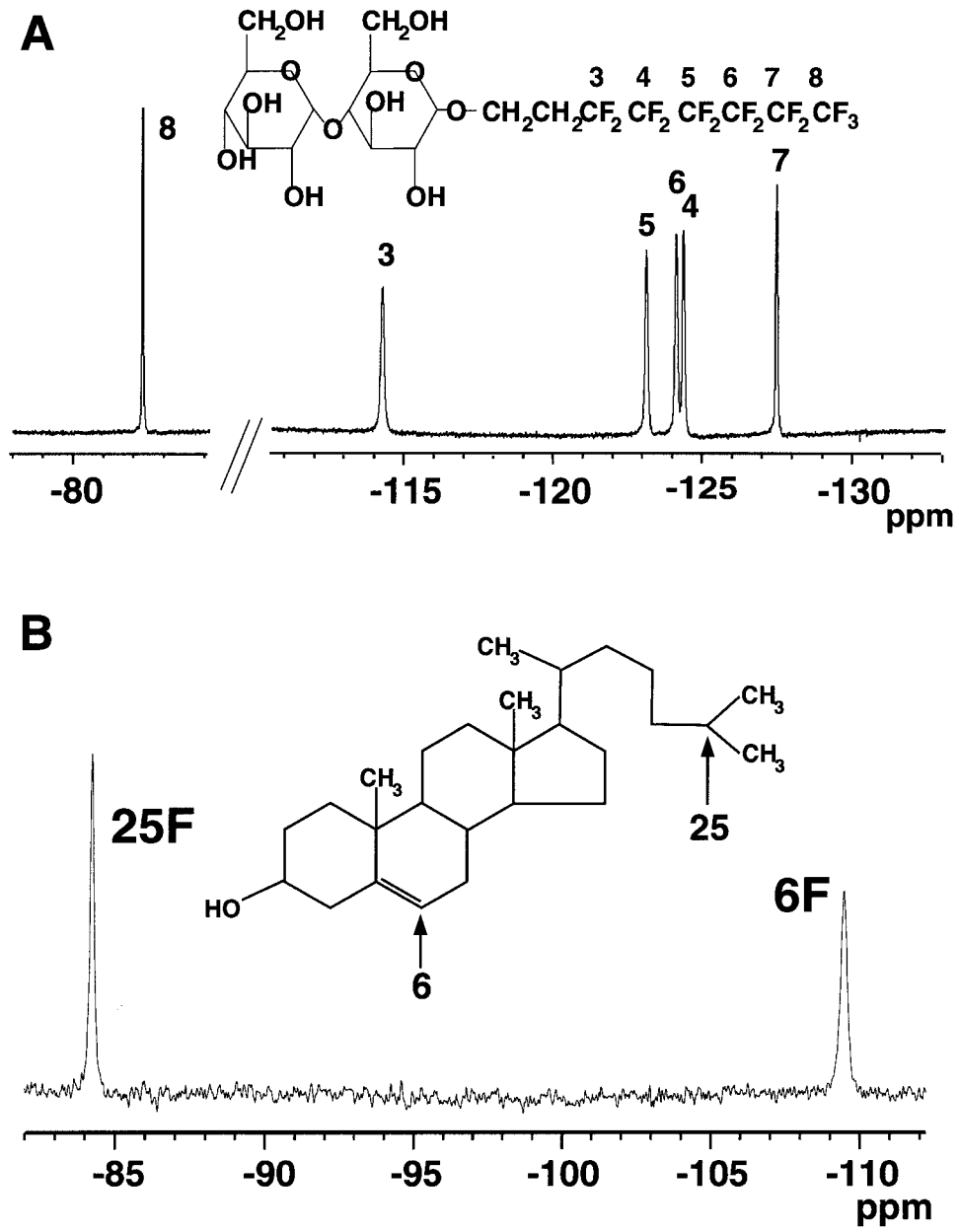

FIGURE 2 (*A*) Structural formula of TFOM, showing the labeled positions (3–8) and corresponding ^{19}F NMR spectrum in a 15% (w/w) isotropic bicelle (DMPC/DHPC = 0.5). (*B*) Structural formula of cholesterol, showing the separate labeled positions (6- and 25-F) and corresponding ^{19}F NMR spectrum in a 15% (w/w) isotropic bicelle (DMPC/DHPC = 0.5). The resonances have been referenced externally to trifluoroacetic acid (76.55 ppm).

fluorinated at the 6 and 25 positions. It has recently been shown by measuring the air-water interfacial properties of CH, as 6FCH and 25FCH, and monolayers of POPC containing the cholesterol analogs, using a Langmuir-Pockels surface balance, that the interfacial properties of 6FCH and 25FCH are almost indistinguishable from those of CH (Kauffman et al., 2000). Therefore, it is reasonable to conclude that the disposition of 6FCH and 25FCH in monolayers, bilayers, and isotropic bicelles is very similar to CH. The immersion depth of both the 6 and 25 positions of cholesterol in the bilayer can be reliably estimated, based on earlier experimental and theoretical work (Gabdoulline et al., 1996; Marsan et al., 1999). Therefore, cholesterol should serve as a useful standard for relating relaxation rates to immersion depth. The ^{19}F NMR spectra of TFOM and a sample consisting of both 6FCH and 25FCH, in $q = 0.5$ isotropic bicelles, are shown in Fig. 2, *A* and *B*. The cholesterol spectrum was assigned by simply studying one isotopically labeled species at a time, whereas the TFOM sample was assigned by performing both a (^{19}F,^{19}F) NOESY and double quantum filtered COSY experiment (Prosser et al., 2000). Essentially, a single NOE was identified between positions 8 and 7 in the NOESY experiment on TFOM, whereas the predominant 4-bond couplings connected peaks 3, 5, and 7 in one case and peaks 4, 6, and 8 in the second case.

Paramagnetic dipolar effects in NMR

The effect of paramagnetic oxygen on the above species should include depth-dependent paramagnetic chemical shift changes, line broadening, and relaxation rate enhancement. These paramagnetic effects can be succinctly described in terms of a proportionality constant associated with the local concentration of oxygen, W, the average distance between the nuclear spin and paramagnetic oxygen, $(1/r_{IS}^6)$, and a spectral density term, which includes the nuclear and electronic Larmor frequencies ω_I and ω_S and the effective correlation time τ_S characterizing electron-nuclear coupling. In particular, the paramagnetic dipolar contribution to the nuclear spin-lattice relaxation rate, R_1^P, and the paramagnetic dipolar spin-spin relaxation rate, R_2^P, can be expressed as follows (Kimmich and Peters, 1975; Peters et al., 1996):

$$R_1^P = W\frac{2}{15}\left(\frac{\mu_0}{4\pi}\right)^2\frac{\gamma_I^2\mu_{eff}^2\beta^2}{r_{IS}^6}\left(\frac{3\tau_S}{1+\omega_I^2\tau_S^2}+\frac{7\tau_S}{1+\omega_S^2\tau_S^2}\right) \quad (1)$$

$$R_2^P = W\frac{1}{15}\left(\frac{\mu_0}{4\pi}\right)^2\frac{\gamma_I^2\mu_{eff}^2\beta^2}{r_{IS}^6}\left(4\tau_S+\frac{3\tau_S}{1+\omega_I^2\tau_S^2}+\frac{13\tau_S}{1+\omega_S^2\tau_S^2}\right), \quad (2)$$

where γ_I represents the nuclear gyromagnetic ratio, μ_{eff} is the effective magnetic moment of the paramagnetic species and β is the Bohr magneton. The correlation time in the above expression, τ_S, is defined by the electronic relaxation time T_{1e}, the residence time of the oxygen species near the nuclear spin τ_{ex} and the effective motional correlation time of the molecule (in this case, TFOM) under study, τ_R, such that (Peters et al., 1996)

$$\frac{1}{\tau_S}=\frac{1}{T_{1e}}+\frac{1}{\tau_{ex}}+\frac{1}{\tau_R}. \quad (3)$$

The above expressions for R_1^P and R_2^P are graphed as a function of τ_S in Fig. 3, using a Larmor frequency, ω_S corresponding to that for ^{19}F at 500-MHz field strengths (470.38 MHz). Note that the paramagnetic spin-lattice relaxation rate is observed to be most effective when τ_S is on the order of 3×10^{-10} s, whereas paramagnetic line-broadening effects become significant for correlation times longer than this limit. In principle, relaxation-effective intramolecular processes might be expected to contribute to the spin-lattice relaxation rates (i.e., $1/\tau_R > 1/\tau_{ex}, 1/T_{1e}$). In this case, the above paramagnetic relaxation rates would depend on local mobility and would therefore not necessarily reflect membrane immersion depth. However, the electronic relaxation time T_{1e} of oxygen is on the order of 10^{-11} s such that the correlation time is determined principally by T_{1e} (i.e., $1/\tau_S \approx 1/T_{1e}$ and $1/T_{1e} > 1/\tau_{ex}, 1/\tau_R$). The second possibility is that the contribution to $1/\tau_S$ is dominated by exchange. Using estimates for the diffusion rate of

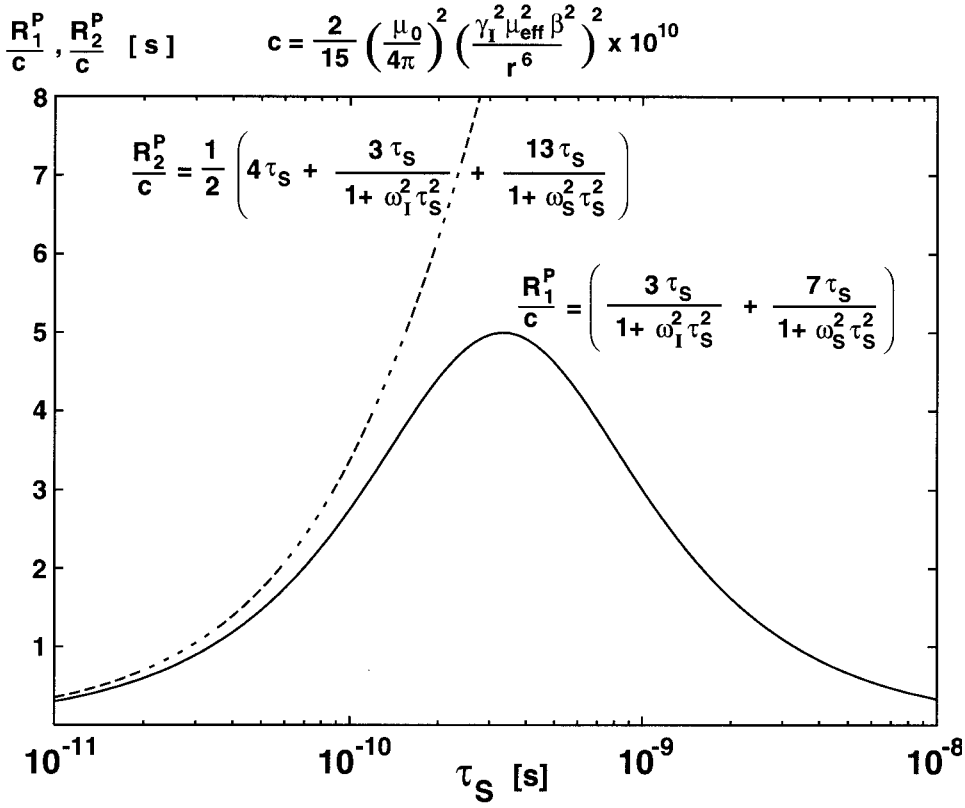

FIGURE 3 Dipolar paramagnetic relaxation rates R_1^P and R_2^P as a function of the correlation time τ_S. The Larmor frequencies $\omega_I = 3.0 \times 10^9 s^{-1}$ and $\omega_S = 3.8 \times 10^{12}\ s^{-1}$ apply to ^{19}F nuclei and electrons, respectively, at 500-MHz NMR field strengths.

oxygen in membranes obtained by Windrem and Plachy (1980), exchange times τ_{ex} on the order of 3×10^{-11} s are possible. In either case, the effect of intra- or intermolecular motions on the paramagnetic relaxation rates is minimized. This is an important advantage over other paramagnetic probes because the correlation time τ_S is either expected to be the same throughout the membrane (if dominated by the electronic spin-lattice relaxation rate) or vary monotonically with immersion depth (if dominated by exchange through oxygen diffusion). Therefore, the paramagnetic relaxation rates will depend only on $1/r_{IS}^6$ and the local (depth-dependent) concentration coefficient of oxygen, W. Note that the electronic relaxation time of typical membrane nitroxide paramagnetic spin labels is between 700 and 1500 ns (Koptyug et al., 1996). In this case, it is clear from the predicted spin-lattice relaxation rate curve in Fig. 3 that if there are exchange processes or intramolecular (depth-dependent) relaxation-effective motions, whose correlation times are less than T_{1e}, then it would be difficult to interpret the relaxation rate in terms of depth.

The spin-lattice relaxation rate R_1 can be easily determined at any oxygen concentration by a simple inversion-recovery measurement. To measure the paramagnetic contribution to this spin-lattice relaxation rate, R_1^P, it is necessary to subtract the observed spin-lattice relaxation rate of a degassed sample, R_1^0, from R_1. To separate pressure effects from paramagnetic effects, one can also measure the relaxation rate under an equivalent partial pressure of nitrogen. This gives essentially the same result and has been reported in an earlier paper (Prosser et al., 2000). Fig. 4 *A* compares both the relaxation rates of TFOM at ambient pressures (after degassing) to the paramagnetic rates under 100 Atm oxygen partial pressure, as a function of chain position. R_1^0 is shown to decrease from nearly 5 s^{-1} at position 3 to 2 s^{-1} at the trifluoromethyl position. In contrast, the paramagnetic relaxation rates, R_1^P, at 100 Atm range from roughly 52 s^{-1} to 75 s^{-1} and are exquisitely sensitive to chain position. Chemical shift changes at 100 Atm also proved to be equally sensitive to chain position, as shown in Fig. 4 *B*. These shifts are accompanied by oxygen-induced line broadening. For example, the trifluoromethyl line width at position 8 is observed to increase from roughly 20 Hz at ambient pressure to 50 Hz, under 100 Atm oxygen partial pressure. The remainder of the ^{19}F NMR line widths (positions 3–7) increase on average from 44 to 74 Hz, with no obvious chain-position-dependent or depth-dependent trends. Though line broadening is significant, it should be emphasized that 50 Hz corresponds to 0.1 ppm at 470 MHz, whereas the chemical shift changes range between 4 and 7 ppm. Thus, chemical shift changes are useful indicators of relative immersion depth. The paramagnetic contribution to chemical shifts is dominated by a simple dipolar expression that includes a distance term, involving r_{IS} as above, and a geometric term, involving the orientation θ of the symmetry

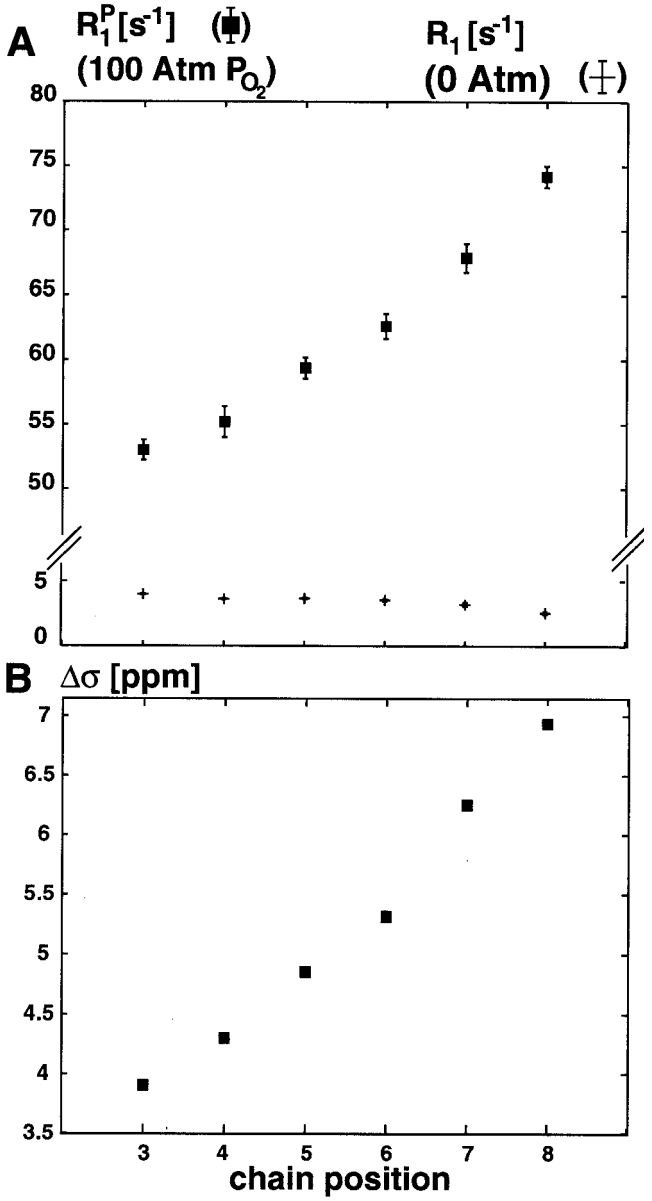

FIGURE 4 Profile of ^{19}F paramagnetic spin-lattice relaxation rates R_1^P and chemical shift changes $\Delta\sigma$ as a function of chain position for TFOM in an isotropic $q = 0.5$ bicelle at 40°C. + represent the relaxation rates, R_1, at ambient oxygen concentrations.

axis of the g-tensor and r_{IS}. Thus (Saterlee, 1990; Peters et al., 1996),

$$\Delta\nu/\nu = W\frac{\beta^2 S(S+1)}{9kT}(g_{\parallel}^2 - g_{\perp}^2)\frac{1-3\cos^2\theta}{r_{IS}^3}, \qquad (4)$$

where $\beta = eh/2mc$, S is the spin of the paramagnetic species, and $g_{\parallel}$ and $g_{\perp}$ are familiar electronic g-tensor quantities. Note that the paramagnetic relaxation rates are predicted to depend on $1/r_{IS}^6$, whereas the chemical shift changes are predicted to depend on $1/r_{IS}^3$ and therefore both

measurements complement each other in assessing diffusional accessibility of oxygen.

Pressure dependence of paramagnetic effects

Because higher oxygen partial pressures result in higher paramagnetic relaxation rates, it is useful to estimate at what pressure the experiment is most sensitive (i.e., at what pressure are the paramagnetic relaxation rates or chemical shift changes most differentiated as a function of immersion depth?). The concentration of molecular oxygen in the membrane, $C^{M}_{O_2}$, is given by Henry's law (at least up to partial pressures of 100 Atm) and may be expressed in terms of a partition coefficient K_p between the membrane and water, such that

$$C^{M}_{O_2} = K_p \alpha_H P_{O_2}, \quad (5)$$

where α_H is Henry's Law constant (5.9×10^{17} Atm^{-1} cm^{-3}). Using a membrane partition coefficient of 2.9 (Kimmich and Peters, 1975), the concentration of molecular oxygen in the membrane, at a partial pressure of 100 Atm, is estimated to be 1.8×10^{20} cm^{-3}, or 22.5% of the concentration of the lipids. Thus, higher pressures translate directly into larger relaxation rates. However, to better differentiate paramagnetic relaxation rates, R^{P}_1, or chemical shift changes, the application of higher oxygen partial pressure should have the effect that relatively more oxygen partitions into the middle of the hydrophobic domain of the bilayer. This effect is clearly observed in Fig. 5 where the pressure dependence of the spin-lattice relaxation rates is given for each chain position in TFOM. At lower pressures, this dependence is roughly linear in accordance with Henry's law. However, the slope of each line is observed to increase with chain position, indicating that the diffusional accessibility gradient of oxygen becomes proportionately higher, with greater pressures. In other words, a higher proportion of oxygen is found in the hydrophobic interior of the membrane in addition to a larger oxygen gradient with higher pressures. These slopes, which range from 0.84 s^{-1} Atm^{-1} for position 3 to 1.4 s^{-1} Atm^{-1} for position 8, as shown in Table 1, translate directly into greater sensitivity and depth resolution at higher pressures. This effect seems to be saturated at higher partial pressures, as evidenced by the quadratic term in Fig. 5, which ranges from -0.003 s^{-1} Atm^{-2} for position 3 to -0.006 s^{-1} Atm^{-2} for position 8. At higher pressures, membranes are expected to become more ordered, resulting in increased bilayer thickness and reduced area per lipid (Braganza and Worcester, 1986). The ordering effect, which reduces the number of defects and diffusional accessibility of oxygen, is progressively greater toward the lipid terminal methyl positions. This is reflected by the above quadratic terms, whose magnitudes increase toward the membrane interior. It should be emphasized that despite the pressure-dependent change in the oxygen profile, this ordering effect must be very slight at 100 Atm because earlier studies in membranes reveal almost no

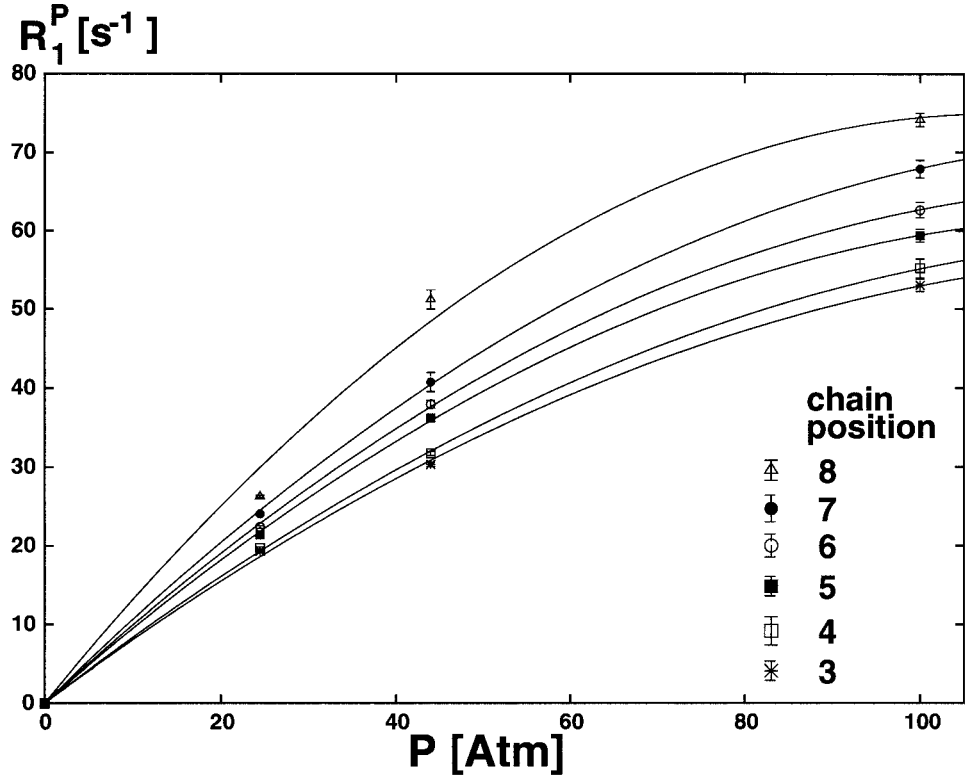

FIGURE 5 Paramagnetic relaxation rates (R^{P}_1) of TFOM in an isotropic $q = 0.5$ bicelle as a function of oxygen partial pressure. The solid lines indicate fits of R^{P}_1 for each chain position, assuming a quadratic pressure dependence (see Table 1).

TABLE 1 Quadratic fit of pressure dependence of paramagnetic spin-lattice relaxation rates, R_1^P, of TFOM

Chain	a (s^{-1} Atm^{-2})	b (s^{-1} Atm^{-1})
3	−0.0031	0.84
4	−0.0032	0.87
5	−0.0039	0.99
6	−0.0041	1.03
7	−0.0043	1.11
8	−0.0064	1.38

The parameters in the table, correspond to a and b, where $R_1^P = aP^2 + bP$.

changes in lipid order parameters at 100 Atm (Bonev and Morrow, 1995).

The optimal sensitivity should occur where we observe the greatest range of relaxation rates. By fitting the pressure dependence of the relaxation rates, for each chain position, to a quadratic (i.e., $R_1^P = aP^2 + bP$) we can estimate the pressure where the greatest difference in relaxation rates occurs. This analysis predicts a maximum near 100 Atm. For other samples, or indeed other nuclei, the optimal pressure may be significantly different from that observed for TFOM. The spin-lattice relaxation rates depend on γ_S^2, and we would therefore expect R_1^P to be most sensitive in (though not necessarily confined to) ^1H or ^{19}F NMR studies. Therefore, higher oxygen concentrations may be necessary to optimize the depth-dependent effect with other nuclei. Line broadening may also be a serious consideration. Although 35-Hz line broadening does not seriously impair our ^{19}F NMR studies, this magnitude of line broadening would be disastrous in some ^1H NMR studies, where the dispersion of most resonances is less than 10 ppm. In our experience, an oxygen partial pressure of 15 Atm is therefore effective in membrane immersion depth studies, using ^1H NMR.

Quantitating immersion depth

Because the paramagnetic spin-lattice relaxation rates are simply proportional to the local concentration of oxygen, it should be possible to estimate this proportionality constant using a well defined fluorinated probe molecule whose position in the membrane can be independently determined. CH was chosen as a probe molecule because it is relatively rigid and its position and orientation are well known in a variety of membranes. In particular, the 25 and 6 positions can be estimated to be separated by roughly 10 Å along the bilayer normal axis, and their rms positions in the membrane can be estimated to be 2 and 12 Å from the bilayer center (Gabdoulline et al. 1996; Marsan et al. 1999), as shown in Fig. 6. The profile of oxygen diffusibility, which has been previously studied by Windrem and Plachy (1980) using ESR and specific spin-labeled lipids, can be approximated as a Gaussian function with a maximum concentration in the middle of the membrane (Fig. 6). Assuming the relaxation is dominated by short-range paramagnetic effects, we can then approximate the relaxation rate profile as Gaussian, such that

$$R_1^P = A \exp\left(\frac{-z^2}{2\sigma^2}\right), \tag{6}$$

where z represents the position, in angstroms, of the nuclear spin of interest, from the center of the membrane. Using the measurements of R_1^P for the 6F and 25F positions of CH in a $q = 1.0$ isotropic bicelle, at 100 Atm, we then determined $A = 78.3\ s^{-1}$ and $\sigma = 14$ Å. In an identical isotropic bicelle system, we then used this distribution to estimate the membrane immersion depth of each fluorinated position of TFOM in the bilayer. There is a slight complication in this analysis because the aliphatic chain possesses an increasing number of gauche conformers toward the trifluoromethyl end. Therefore, the projection of the chain positions along the bilayer normal would be expected to be more closely spaced toward the end of the chain. To account for this, the spacing between successive difluoromethylene groups was assumed to decrease (toward the trifluoromethyl terminus) by some fixed amount, which could be determined by a least-squares fitting of the TFOM relaxation rates to the above Gaussian curve. The maximal spacing was assumed to be between C3 and C4. The result of a least-squares fit of relaxation rates of TFOM to membrane immersion depth using the above Gaussian profile was that the respective chain positions were determined to have membrane immersion depths of 13.3, 11.3, 9.9, 8.6, 7.3, and 5.9 Å from C3 to C8, respectively, as shown in Fig. 6. It is possible to refine the distribution function further by considering an integral or average over cylindrical space of $(1/r_{IS})^3$ or $(1/r_{IS})^6$. However, such an analysis would first require more accurate information regarding the oxygen diffusibility profile.

The relaxation rate dependence on membrane immersion depth depends strongly on the given pressure, as shown above, and on the composition of the model membrane system. In other words, a different range of paramagnetic relaxation rates would be expected for the same molecules in a small unilamellar vesicle system, for example. Therefore, without first employing a standard such as the above specifically fluorinated cholesterol species, the relaxation rates and differential chemical shift changes should only be used to determine relative immersion depth. Recently, we have begun investigating the positional and orientational properties of an antibacterial peptide, indolicidin, whose primary sequence is ILPWKWPWWPWRR-NH_2. The structure of this peptide has recently been determined by high-resolution NMR in detergent micelles (Rozek et al., 2000). At issue is the exact position and orientation of this peptide in a membrane bilayer. To address this, we have employed an indolicidin analog, in which Trp-8 and Trp-9 have been separately replaced with 5-fluorotryptophan. The high-resolution NMR results of Rozek and co-workers sug-

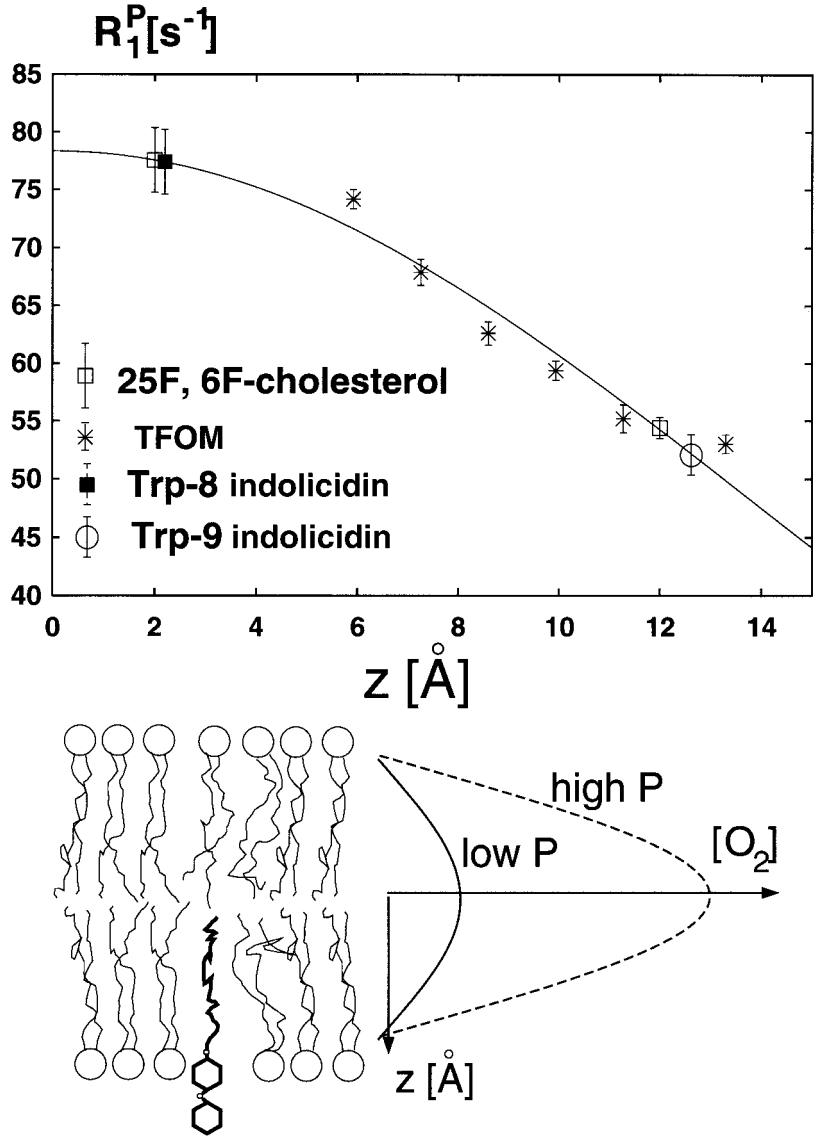

FIGURE 6 The paramagnetic relaxation rate R_1^P as a function of membrane immersion depth in an isotropic $q = 0.5$ bicelle at 100 Atm oxygen partial pressure. $z = 0$ Å defines the middle of the hydrophobic interior, as indicated in the illustration, and the solid line represents a fit of the data for specifically fluorinated cholesterol, TFOM, and two specifically fluorinated peptide (indolicidin) analogs to a single Gaussian. Note that an increase in pressure results in a larger oxygen gradient and, therefore, greater depth resolution, as implied by the lower figure.

gested that indolicidin was roughly banana-shaped with the middle of the banana (at residue 8) buried most deeply in the membrane (Rozek et al., 2000). It is interesting to note that 5-fluorotryptophan alone is observed to intercalate into membrane bilayers and a paramagnetic spin-lattice relaxation rate of 37.8 ± 0.3 s^{-1} was measured in $q = 0.5$ bicelles at 100 Atm, indicating clearly that the 5-fluoro position of tryptophan alone is slightly immersed in the hydrophobic domain (for comparison, R_1^P is observed to be 12.4 s^{-1} at 100 Atm for 5-fluorotryptophan in water alone). The relaxation rate of this same label, as part of the indolicidin peptide, is observed to be 78 s^{-1}, in an isotropic bicelle, at the same temperature and pressure, whereas the ^{19}F NMR resonance is shifted downfield by 4.0 ppm. This suggests that the tryptophan (residue 8 on indolicidin) is anchored in the bilayer, with the specific fluorine nucleus lying nearly in the center of the bilayer, consistent with the model put forth by Rozek and co-workers. This may be contrasted with the paramagnetic relaxation rate for 5-fluorotryptophan at residue 9, which is estimated to lie 11 Å from the from the bilayer interior, according to the relaxation curve in Fig. 6. This finding, which is in agreement with the prediction of Rozek et al. (2000), allows us to determine the positioning of the peptide in the membrane and will be discussed in greater detail in a subsequent paper.

CONCLUSIONS

The results presented in this paper show that chemical shift changes and paramagnetic spin-lattice relaxation rates are sensitive indicators of membrane immersion depth. These results may be contrasted with the recent work of Teng and Bryant (2000), who used paramagnetic oxygen to probe

molecular accessibility in a water-soluble protein by NMR. In this work the authors were able to identify regions of molecular accessibility to molecular oxygen through paramagnetic spin-lattice relaxation rates. In membranes, the hydrophobic interior is much less heterogeneous than the interior of a water-soluble protein and therefore affords the possibility of measuring immersion depth and topology of membrane proteins.

Depending on the size of the membrane protein (or importance of using lipid bilayers over detergent micelles) one may choose to use high-resolution NMR in detergent micelles or SS NMR in oriented bilayers to determine three-dimensional protein structure. SS NMR experiments may involve the measurement of particular anisotropic interactions, such as chemical shift anisotropies, quadrupolar or dipole splittings, of appropriately chosen isotopic labels. Alternatively, structural and orientational information may be obtained from uniformly labeled proteins, through experiments such as polarization inversion spin exchange at the magic angle (PISEMA), which correlate ^{15}NH dipole couplings with both ^{15}N and ^{1}H chemical shifts (Ramamoorthy et al., 1995). High-resolution NMR-derived structures rely largely on ^{13}C chemical shifts, scalar couplings, and NOEs. In either case, information on membrane protein topology and the exact positioning of the molecule in the membrane bilayer is critical to the final structural model. The determination of relative immersion depth through paramagnetic broadening or changes in spin-lattice relaxation rates is often achieved in both high-resolution and SS NMR by addition of specific paramagnetic spin labels (proxyl or nitroxide). Fatty acid probes whose spin labels are located either in the headgroup or at specific positions on the aliphatic chain are frequently used for such purposes. The use of paramagnetic oxygen as proposed in this paper presents several advantages over these conventional paramagnetic spin labels. First, the electronic relaxation time of oxygen is sufficiently low that most intramolecular motions do not complicate the analysis. Consequently, line-broadening effects are relatively small. Second, the optimal concentration of oxygen for paramagnetic effects can be easily adjusted by application of appropriate partial pressure. Moreover, this concentration may be considerably higher than that used with nitroxide or proxyl ESR spin labels. Third, oxygen is small in comparison with ESR spin labels and therefore is expected to offer few perturbations of membrane protein structure. Fourth, oxygen can be easily removed or added to the sample. And fifth, oxygen possesses a significant concentration gradient in the membrane. Therefore, a gradient of paramagnetic effects are observed with immersion depth, and it is not necessary to employ a large number of depth-specific spin labels.

The proposed experiments bear a strong similarity to the ESR experiments, originally put forth by Altenbach et al. (1990). The ESR experiments, which also measure relative immersion depth, make use of the contrasting effects of both oxygen and a water-soluble probe such as nickel. The combination of the proposed NMR experiments with oxygen, under pressure, and water-soluble paramagnetic shift reagents such as Eu^{3+} would certainly be useful to determine topology of portions of the membrane protein that is at the membrane-water interface. As shown in this paper, under high pressure, oxygen-induced chemical shift changes and spin-lattice relaxation rates are exquisitely sensitive indicators of relative immersion depth. It is also possible to interpret these paramagnetic relaxation rates, resulting from the addition of oxygen, in terms of an actual immersion depth. In combination with site-directed mutagenesis, ESR has been useful in elucidating membrane protein topology and low-resolution structure. Oxygen not only possesses a well-known concentration gradient across a membrane, but in the case of channel proteins, oxygen-induced paramagnetic effects can clearly be used to discriminate the difference between the inside and outside of a protein. Moreover, at high partial pressures, the oxygen gradient and consequent depth resolution is significantly enhanced. Such gradients are nearly impossible to take advantage of in ESR experiments because ESR spectra are severely hampered by paramagnetics such as oxygen with relaxation rates less than 10^{-9} s (Saterlee, 1990). Therefore, it is possible that at high oxygen partial pressures, NMR may provide unprecedented depth resolution and topological information for membrane proteins.

R.S.P. gratefully acknowledges Research Corporation (RI0322) for making this research possible. We also thank Ad Bax and Chris Roe for kindly loaning us the high-pressure sapphire NMR tubes. Marcia Malmer is acknowledged for the synthesis and purification of 6FCH and 25FCH. We also thank the Nucleic Acids Protein Services (NAPS) unit at UBC for synthesizing the indolicidin peptide analogs.

REFERENCES

Altenbach, C., T. Marti, H. G. Khorana, and W. L. Hubbell. 1990. Transmembrane protein-structure: spin labeling of bacteriorhodopsin mutants. *Science.* 248:1088–1092.

Altenbach, C., D. A. Greenhalgh, H. G. Khorana, and W. L. Hubbell. 1994. A collision gradient-method to determine the immersion depth of nitroxides in lipid bilayers: application to spin-labeled mutants of bacteriorhodopsin. *Proc. Natl. Acad. Sci. U.S.A.* 91:1667–1671.

Becker, E. D. 2000. High Resolution NMR. Academic Press, San Diego.

Bonev, B. B., and M. R. Morrow. 1995. Hydrostatic pressure-induced conformational changes in phosphatidylcholine headgroups: a ^{2}H NMR study. *Biophys. J.* 69:518–523.

Braganza, L. F., and D. L. Worcester. 1986. Hydrostatic pressure induces hydrocarbon chain interdigitation in single-component phospholipid bilayers. *Biochemistry.* 25:2591–2595.

Brown, L. R., W. Braun, A. Kumar, and K. Wuthrich. 1982. High resolution nuclear magnetic resonance studies of the conformation and orientation of melittin bound to a lipid-water interface. *Biophys. J.* 37: 319–328.

Caffrey, M., and J. Wang. 1995. Membrane-structure studies using x-ray standing waves. *Annu. Rev. Biophys. Biomech.* 24:351–377.

Cavanagh, J., W. J. Fairbrother, A. G. Palmer, III, and N. J. Skelton. 1996. Protein NMR Spectroscopy: Principles and Practice. Academic Press, San Diego.

Chupin, V., J. A. Killian, J. Breg, H. H. J. de Jongh, R. Boelens, R. Kaptein, and B. de Kruijff. 1995. PhoE signal peptide inserts into micelles as a dynamic helix-break-helix structure, which is modulated by the environment. A two-dimensional ^{1}H NMR study. *Biochemistry.* 34:11617–11624.

Danielson, M. A., and J. J. Falke. 1996. Use of ^{19}F NMR to probe protein structure and conformational changes. *Annu. Rev. Biophys. Biomol. Struct.* 25:163–195.

Dauber, W. G., B. Kohler, and A. Roestle. 1985. Synthesis of 6-fluorovitamin D_3. *J. Org. Chem.* 50:2007–2010.

Dettman, H., J. H. Weiner, and B. D. Sykes. 1982. ^{19}F nuclear magnetic resonance studies of the coat protein of bacteriophage M13 in synthetic phospholipid vesicles and deoxycholate micelles. *Biophys. J.* 37: 243–251.

Esposito, G., A. M. Lesk, H. Molinari, A. Motta, N. Niccolai, and A. Pastore. 1992. Probing protein structure by solvent perturbation of nuclear magnetic resonance spectra. Nuclear magnetic resonance spectral editing and topological mapping in proteins by paramagnetic relaxation filtering. *J. Mol. Biol.* 224:659–670.

Franklin, J. C., J. F. Ellena, S. Jayasinghe, L. P. Kelsh, and D. S. Cafiso. 1994. Structure of micelle-associated alamethicin from ^{1}H NMR. Evidence for conformational heterogeneity in a voltage-gated peptide. *Biochemistry.* 33:4036–4045.

Gabdoulline, R. R., G. Vanderkooi, and C. Zheng. 1996. Comparison of the structures of dimyristoylphosphatidylcholine in the presence and absence of cholesterol by molecular dynamics simulations. *J. Phys. Chem.* 100:15942–15946.

Gerig, J. T.. 1994. Fluorine NMR of proteins. *Prog. NMR Spectrosc.* 26:293–370.

Harte, R. A., S. J. Yeaman, J. McElhinney, C. J. Suckling, B. Jackson, and K. E. Suckling. 1996. Effects of novel synthetic sterol probes on enzymes of cholesterol metabolism in cell-free and cellular systems. *Chem. Phys. Lipids.* 83:45–59.

Hubbell, W. L., and C. Altenbach. 1994. Investigation of structure and dynamics in membrane-proteins using site-directed spin-labeling. *Curr. Opin. Struct. Biol.* 4:566–573.

Hubbell, W. L., H. S. Mchaourab, C. Altenbach, and M. A. Lietzow. 1996. Watching proteins move using site-directed spin labeling. *Structure.* 4:779–783.

Jeener, J., B. H. Meier, P. Bachmann, and R. R. Ernst. 1979. Investigation of exchange processes by two-dimensional NMR spectroscopy. *J. Chem. Phys.* 71:4546–4553.

Katsaras, J. 1995. X-ray-diffraction studies of oriented lipid bilayers. *Biochem. Cell Biol.* 73:209–218.

Kauffman, J. M., P. W. Westerman, and M. C. Carey. 2000. Fluorocholesterols, in contrast to hydoxysterols, exhibit interfacial properties similar to cholesterol. *J. Lipid Res.* 41:991–1003.

Kimmich, R., and A. Peters. 1975. Solvation of oxygen in lecithin bilayers. *Chem. Phys. Lipids.* 14:350–362.

Knott, R. B., and B. P. Schoenborn. 1986. Quantitation of water in membranes by neutron-diffraction and x-ray techniques. *Methods Enzymol.* 127:217–229.

Koptyug, I. V., S. H. Bossmann, and N. J. Turro. 1996. Inversion-recovery of nitroxide spin labels in solution and microheterogeneous environments. *J. Am. Chem. Soc.* 118:1435–1445.

Lohner, K., and E. J. Prenner. 1999. Differential scanning calorimetry and x-ray diffraction studies of the specificity of the interaction of antimicrobial peptides with membrane-mimetic systems. *BBA Biomembr.* 1462:141–156.

Marsan, M. P., I. Muller, C. Ramos, F. Rodriguez, E. J. Dufourc, J. Czaplicki, and A. Milon. 1999. Cholesterol orientation and dynamics in dimyristoylphosphatidylcholine bilayers: a solid state deuterium NMR analysis. *Biophys. J.* 76:351–359.

McIntosh, T. J. 1999. Structure and physical properties of the lipid membrane. *Curr. Top. Membr.* 48:23–47.

Papavoine, C. H. M., R. N. H. Konings, C. W. Hilbers, and F. J. M. Van De Ven. 1995. Location of M13 coat protein in sodium dodecyl sulfate micelles as determined by NMR. *Biochemistry.* 33:12990–12997.

Peters, J. A., J. Huskens, and D. J. Raber. 1996. Lanthanide induced shifts and relaxation rate enhancements. *Prog. NMR Spectrosc.* 28:283–350.

Prosser, R. S., P. A. Luchette, and P. W. Westerman. 2000. Using O_2 to probe membrane immersion depth by ^{19}F NMR. *Proc. Natl. Acad. Sci U.S.A.* 97:9967–9971.

Ram, P., and J. H. Prestegard. 1988. Magnetic field-induced ordering of bile salt/phospholipid micelles: new media for NMR structural investigations. *Biochim. Biophys. Acta.* 940:289–294.

Ramamoorthy, A., C. H. Wu, and S. J. Opella. 1995. 3-Dimensional solid-state NMR experiment that correlates the chemical shift and dipolar frequencies of two heteronuclei. *J. Magn. Reson. B.* 107:88–90.

Rozek, A., C. L. Friedrich, and R. E. W. Hancock. 2001. Structure of the bovine antimicrobial peptide indolicidin bound to dodecylphosphocholine and sodiumdodecylsulfate micelles. *Biochemistry.* In press.

Sanders, C. R., B. J. Hare, K. P. Howard, and J. H. Prestegard. 1994. Magnetically-oriented phospholipid micelles as a tool for the study of membrane-associated molecules. *Prog. Nucl. Magn. Reson. Spectrosc.* 26:421–444.

Sanders, C. R., and J. H. Prestegard. 1990. Magnetically orientable phospholipid-bilayers containing small amounts of a bile-salt analog, CHAPSO. *Biophys. J.* 58:447–460.

Sanders, C. R., and R. S. Prosser. 1998. Bicelles: a model membrane system for all seasons? *Structure.* 6:1227–1234.

Sanders, C. R., and J. P. Schwonek. 1992. Characterization of magnetically orientable bilayers in mixtures of dihexanoylphosphatidylcholine and dimyristoylphosphatidylcholine by solid-state NMR. *Biochemistry.* 31: 8898–8905.

Saterlee, J. D. 1990. Fundamental concepts of NMR in paramagnetic systems. *Concepts Magn. Reson.* 2:69–79.

Steinhoff, H. J., R. Mollaaghababa, C. Altenbach, H. G. Khorana, and W. L. Hubbell. 1995. Site-directed spin-labeling studies of structure and dynamics in bacteriorhodopsin. *Biophys. Chem.* 56:89–94.

Sykes, B. D., and W. E. Hull. 1978. Fluorine nuclear magnetic resonance studies of proteins. *Methods Enzymol.* 49:270–295.

Teng, C. L., and R. G. Bryant. 2000. Experimental measurement of nonuniform dioxygen accessibility to ribonuclease A surface and interior. *J. Am. Chem. Soc.* 122:2667–2668.

Vold, R. R., R. S. Prosser, and A. J. Deese. 1997. Isotropic solutions of phospholipid bicelles: a new membrane mimetic for high-resolution NMR studies of polypeptides. *J. Biomol. NMR.* 9:329–335.

Windrem, D. A., and W. Z. Plachy. 1980. The diffusion-solubility of oxygen in lipid bilayers. *Biochim. Biophys. Acta.* 600:655–665.